Multiphysics SPH simulation of flow drilling process

Anthony Journaux[1], Tess Legaud[1], Vincent Lapoujade[1]

[1] DynaS+, 5 avenue Didier Daurat 31400 TOULOUSE France, a.journaux@dynasplus.com

1   Abstract

Flow drilling is an alternative drilling solution for metal plates up to several centimeters. Using a conical tool, the process combines high rotation speed and high pressure to initiate friction and heat up the plate material locally in contact with the tool. As a consequence, the heated material has its mechanical characteristics reduced and is subjected to a very large plastic deformation. The surplus of matter is not wasted but is shaped into a collar above the metal plate and a socket below. These bulges induce a local additional thickness enabling a direct threading without added parts (bolt...).

Flow drilling technology has emerged since 1923 but has been little used due to the inherent difficulty to accurately predict the collar size and extent. The process itself is mature and used sparsely in the industry but is lacking a numerical tool able to simulate accurately the thermal and mechanical effects in order to ensure a reliable procedure.

Flow drilling is by nature a multiphysics process which also leads to locally high deformation. Such complex phenomena can be addressed by LS-DYNA which offers the possibility to couple Multiphysics solvers and the use of SPH method to deal with large deformations in continuous material.

The work undertaken and presented in this paper follows three steps of increasing complexity:
- Build a SPH model of the process using a purely mechanical solver with a pseudo-thermal model using steel materials with an idealized thermal gradient
- Evaluate the compatibility between SPH modelling and the LS DYNA thermal solver and ensure the friction, dilatation and diffusion work properly together with a SPH model.
- Set up a coupled mechanical-thermal model able to simulate the complete process accurately

2   Introduction

2.1   What is flow-drilling

Flow drilling is a process using the friction energy to increase the temperature in a metal in order to locally decrease the material properties in the metal around the tool and easily perforate it. Indeed, using a conical tool, the process combines high rotation speed (1500-5000 rpm) and high force (1000-5000 N) to initiate friction and heat up the plate material locally in contact with the tool. As a consequence, the heated material has its mechanical characteristics reduced and is subjected to very large plastic deformation.

Though the process has been invented in 1923 by Jean Claude de Valière, it became effective only around 1980 when the use of new materials with high thermal and mechanical resistance was common. [1] [2]

This process is used in the automotive industry; but the necessity to conduct costly series of tests to find the best parameters for every case conducts the industry to use this process only for mass production.
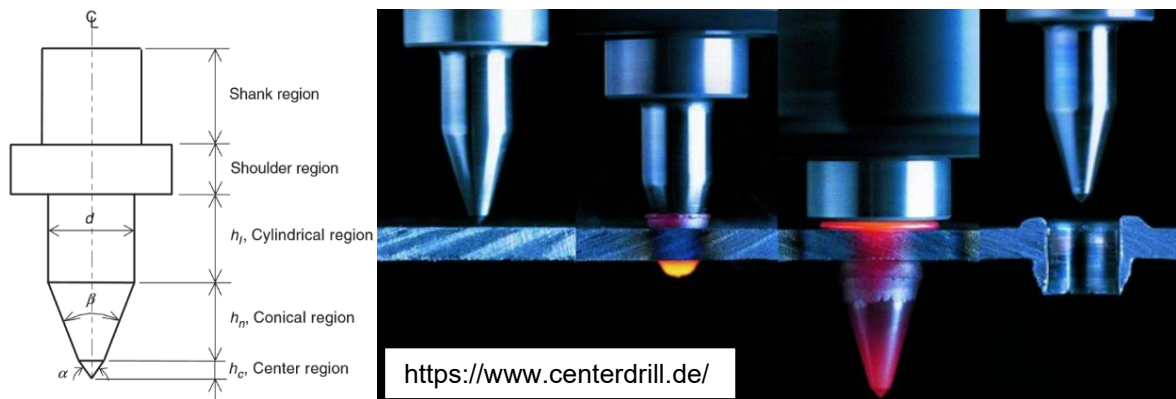

Fig.1:   Cutting plan of a standard tool (left) and the different steps of the process (right)

2.2   Advantages and drawbacks

The surplus of matter is not wasted but is shaped into a collar above the metal plate and a socket below. These bulges induce a local additional thickness enabling a direct threading without added parts (bolt...). The matter undergoes high temperatures and stresses and there is a change in the microstructure of the material which is equivalent to a new heat treatment. Thus, the matter around the hole can have new mechanical characteristics.[3] The process itself last between 2 and 6 seconds and works with many metals.

However, the process is available only for plates with relatively small thicknesses (10 mm maximum) and the diameter of the drilling should be at least two times superior to the thickness. The process needs a powerful machine (1.5 – 5 kW) to complete. Last but not least, the process is complex to simulate and is lacking a numerical tool able to simulate accurately the thermal and mechanical effects in order to ensure a reliable procedure.

2.3   Goal of this study

Flow drilling is by nature a multiphysics process which also leads to locally high deformations. Such complex phenomena can be addressed by LS-DYNA which offers the possibility to couple Multiphysics solvers and the use of SPH method to deal with large deformation in continuous material.

As the machine resources dedicated for this study will be moderate (28 CPU) and in order to keep a reasonable processing time; the global goal is to demonstrate the feasibility of a simulation of flow drilling using LS-DYNA without the necessity of making an accurate model of the reality but rather a simplified model in order to bring a proof of concept and analyze the qualitative results.

The work undertaken and presented in this paper follows three steps of increasing complexity:

- Build a SPH model of the process using a purely mechanical solver with a pseudo-thermal model using steel materials with an idealized thermal gradient,
- Evaluate the compatibility between SPH modelling and the LS DYNA thermal solver and ensure the friction, dilatation and diffusion work properly together with a SPH model,
- Set up a coupled mechanical-thermal model able to simulate the complete process accurately.

3   Mechanical approach

In this first step, the aim is to realize a preliminary simulation without using any thermal tool and solver in order to highlight the issues that will be encountered by simulating flow drilling.

3.1   Model simplifications

The first issue is to correctly simulate the heavy plastic deformations involved; such deformations cannot simply be simulated by a standard Lagrangian Mesh. Both ALE and SPH methods are potential candidates to simulate these high deformations. As the ALE method would lead to several drawbacks: the size of the model would be important due to the necessity to mesh accurately a big volume which doesn't include any matter. Furthermore, we don't want to deal with the potential lack of accuracy and conservativity and the diffusive aspect associated with the ALE scheme. Instead for this POC work, we choose to use the SPH method (Smoothed Particule Hydrodynamics) in our model as we thought the main drawbacks of this method (the tension instability) easier to cope with.
According to the internal experience at DynaS+, the distance between the SPH elements must be the same in all directions in order to have a correct accuracy, and it is also necessary to have at least around 10 elements in the smaller dimension. Thus, both the number of SPH elements and the inter-particular distance are established by the thickness of the plate. Consequently, dividing by 2 the distance between the SPH elements is equivalent, all others things being equal, to multiplying by 8 the number of elements and to dividing by 2 the timestep. Then, the processing time is roughly multiplied by 16.

Besides, the model can't be symmetrized and the whole model has to be modelized.

Furthermore, the duration of the process is slow (6-10 seconds) in regard with the order of magnitude of the timestep. High number of elements, low timestep and slow process causes the processing time to be excessively high. In order to reduce this processing issue, the model will be simplified with two major changes:
- In reality, the thickness of the plate is rather thin (usually around 2 mm) but the model will represent a plate 5 mm thick; dividing the processing time by roughly 40 (i.e. $(2.5)^4 \approx 39$)
- The speeds of the process are multiplied by 50 in regard of the reality, in order to reduce the processing time and quickly perform the simulations. The rotational and translational speed of the tool in the simulations are respectively 14.4 rad/sec and 0.2 m/sec; dividing the processing time by 50.

Finally, the aim of this model is to represent the weakened properties of the steel around the contact with the tool without using the thermal solver. The gradient of temperature will be considered frozen in time.
A simple thermal study has been made to represent the gradient of temperature at the end of the simulation: a 100*100*5 mm³ plate with S235 steel characteristics has the temperature at the center fixed at 600 °C and everywhere else at 20°C. The simulation last for 6 seconds and the heat propagates from the center during this time. The final gradient of temperature is measured and will be used in the current model.

3.2   Material Law

The plate material is an S235 steel alloy. In this first model, the MAT_24 is used to represent this material with the following characteristics:

The tool material is a tungsten carbide and is considered rigid. As this material possesses high mechanical and thermal resistances, the deformations of the tool are considered negligible with respect to the plate ones. Consequently, the MAT_RIGID is used to represent the tool material.

The data of the annex 1 of the Eurocode 3 part 1-2 on "General rules Structural fire design" are used to represent S235 steel properties at different temperatures. [04]

3.3 Pseudo thermal model

The steel plate measures 100*100*5 mm^3 but only a central square (30 mm long) is meshed with SPH elements. The exterior part (in red) is constituted of solid elements of 1.67mm mesh size. The bottom nodes in the exterior of this part are fixed and a **CONTACT_TIED_NODE_TO_SURFACE** is used between the red part and the blue SPH part.
The tool is rigid. A **CONTACT_AUTOMATIC_NODE_TO_SURFACE** is used between the tool shell elements and the SPH nodes.

The number of SPH elements in the depth of the plate is 8. Using 8 rather than 10 SPH elements in the depth allows for a reduction from 64000 to 18400 SPH elements and an increase of the timestep from 200 ns to 250 ns. In total, this operation should reduce the processing time of around 77%.

There are 4 SPH parts, each of them reflects a zone of the temperature gradient in the metal by using different materials. In a 5.5 mm radius around the impact zone of the tool, the material represents S235 steel at 600°C (red part), beyond and in a radius of 7 mm, the material represents S235 steel at 400 °C (yellow part), in a radius of 9 mm, the material represents a S235 steel at 200 °C (green part). Beyond the 9 mm radius, the material is a classical S235 steel at room temperature (blue part).
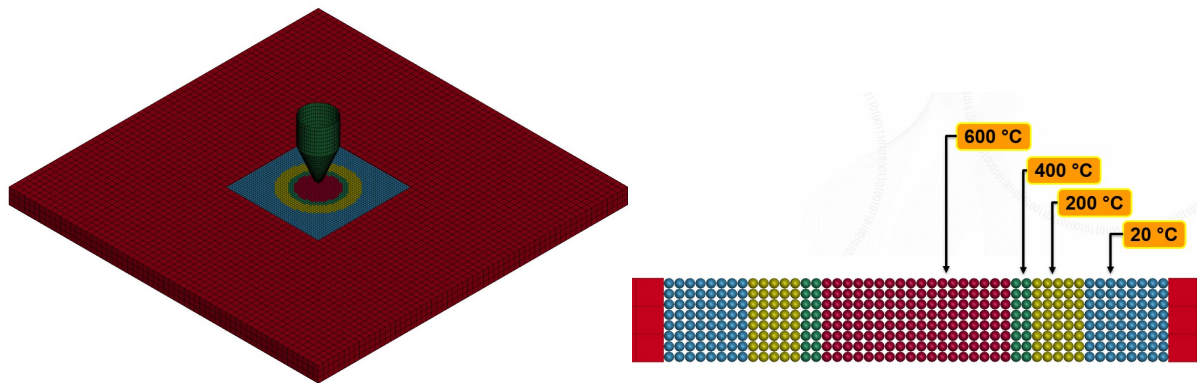

Fig.2: Pseudo-thermal model (left) and temperature gradient in the thermal simulation (right)

In order to have comparative results, the geometry of the tool modelled with shell elements will be shaped in three areas as described on Figure 3.
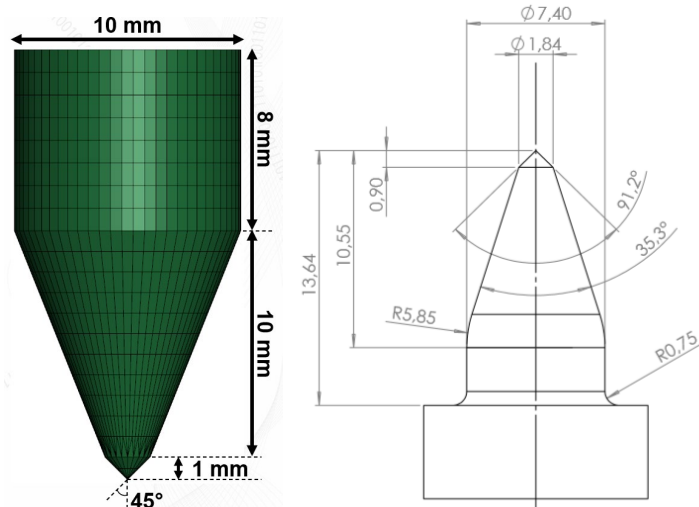

Fig.3: Simplified model (left) and example of a pattern of a tool (right)

This model is still distant from reality for several reasons:
- There is no evolution of the temperature and the steel is arbitrarily warmed up at the beginning of the simulation.
- The translational and rotational speeds of the tool are 50 times higher than reality.
- The thickness of the plate is 5 mm instead of 2 mm.

3.4 Pseudo thermal model results and comparison to experimental results

The simulation works to its end. The results are encouraging, the hole has been drilled and there are several elements to analyze. The Von Mises Stress around the drilling is around 300 MPa with a maximum at 500 MPa. This value is quite high for the process and the deformations are still important far from the drilling, it indicates that the temperatures around the hole aren't high enough to replicate the process and soften the material. In further tests, the temperature at the plate center will be increased to 800°C instead of 600°C.

There is no collar forming on the top of the plate which doesn't represent the reality, it brings to light that the cylindrical gradient of temperature is not the best suited to represent this process as the heating is located at the contact with the tool. Thus, the material being softer on the upper side of the plate, the displaced matter should be pushed through the top rather than to the bottom.
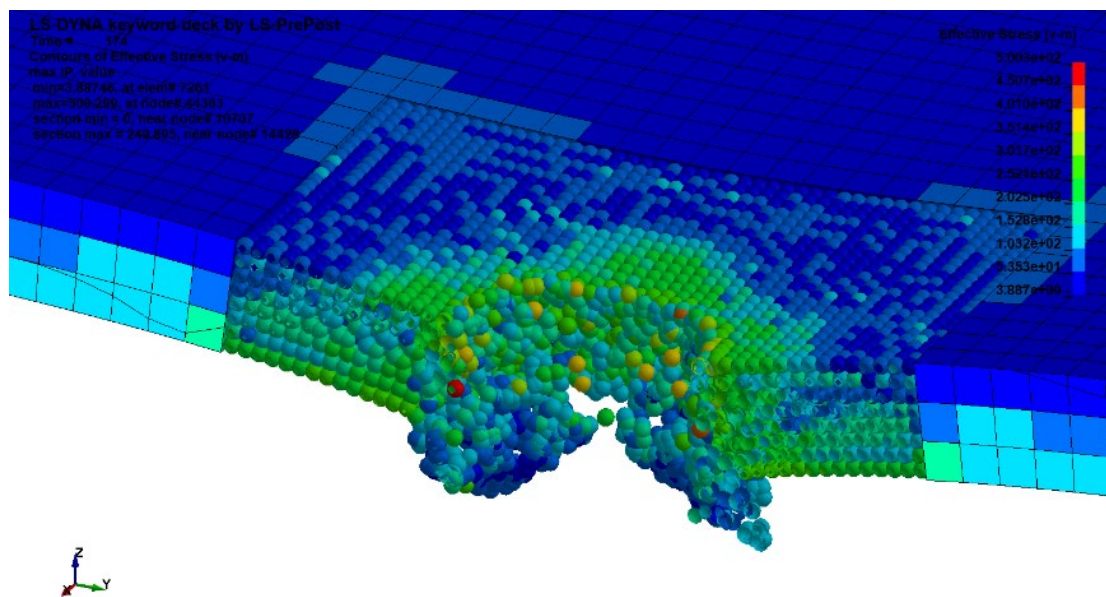

Fig.4: Von Mises stress at the end of the simulation.

3.4.1 Petals

The drilling generates 4 „petals" instead of the smooth socket that is created in reality. Accoring to the litterature [5][6], these petals usually appear with brittle/fragile metals. For example, in the experimentations, flow drilling in an Al380 aluminium alloy plate creates a drill with a rough surface and the inferior ring is bursted in „petals" which go along with cracks which can reach up to the lenght of the ring itself (figure 5).

The ratio thickness of the object on the diameter of the hole has an important influence on the creation of the petals as a low ratio favors the petals and cracks appearance. Oppositely, the faster the displacement goes, the higher the petals and cracks are.

In the simulation, even if the steel shouldn't produce such "petals", their formation along with important cracks seems coherent given the speeds of the tool in the model. Another factor that could encourage the formation of petals is the distribution of the SPH elements.
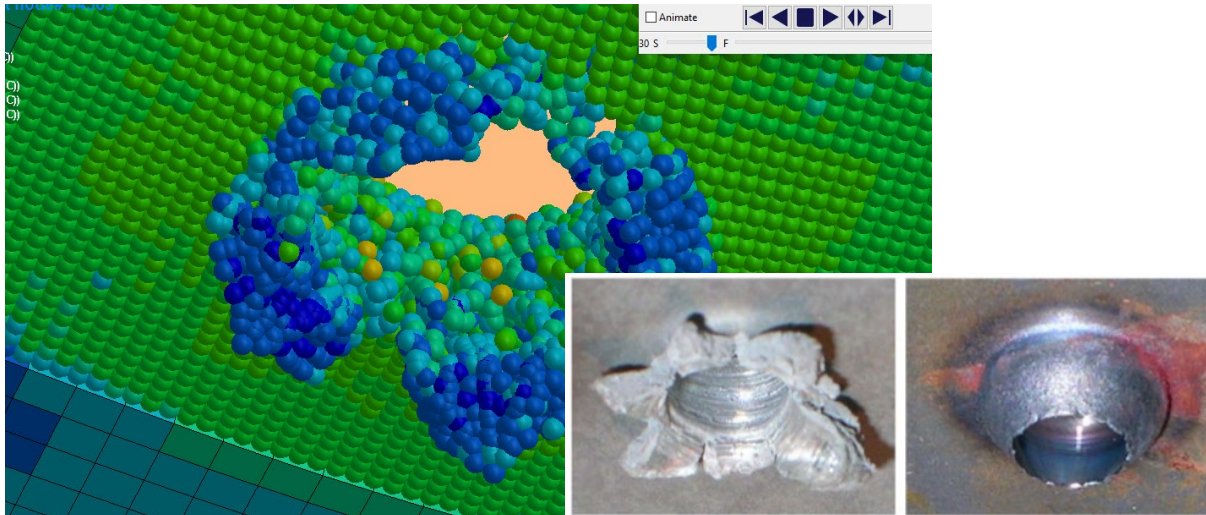
Fig.5: Petals obtain in the standard steel simulation (left) compared to petals obtain with Al380 (bottom left) or with standard steel (bottom right)

3.4.2 Force analysis

The experimental curves, shown below from the literature, highlight that the object temperature, the translational displacement speed and the rotational one has an important influence on the final results. The literature's test has been realized on a plate of 3 mm thickness and the material is an aluminum. [7]

The last spike, in figure 6, is caused by the flattening of the socket on the plate which doesn't happen in the simulation. The first spike occurs around 3 mm of penetration. From this spike, the frictional energy is high enough to quickly heat the material thus reducing the properties of the material; the entry of the tool becoming easier.

The speed of the process being constant, it is possible to compare the aspect of the curve obtained from the simulation to the experimental curves. The aspects of the curves are really different and demonstrate that such simulation is not accurate enough. As the matter doesn't warm up, the matter does not become softer with time and the force necessary to go through the plate is too low at the beginning and too high at the end of the simulation. Thus, the spike is shifted to the right.

In light of these technicalities, even with drastically different parameters, the shape of the simulated curve is coherent. The orders of magnitude of the forces (6 kN for the simulation and around 1-3 kN for the experimental tests) are highly different due to the plate using a softer material and being finer in the literature.
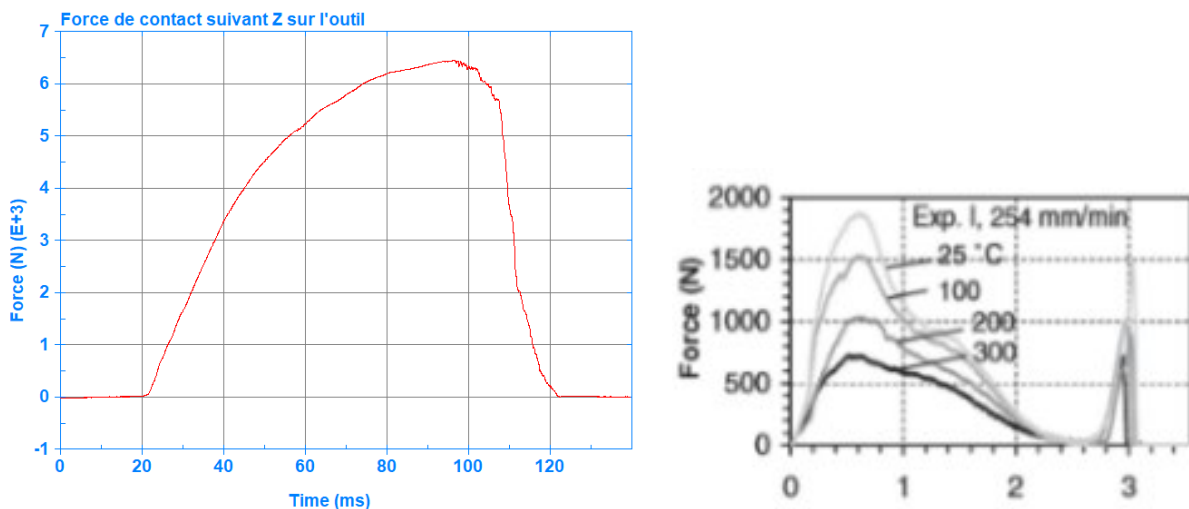

Fig.6: Curve of the simulated thrust force (left) compared to experimental thrust force and torque at different advance speed and pre-heated plate temperature (right)

3.5   Pseudo thermal model with spherical gradient

To improve the model, the temperature gradient is made from material spheres taking into account modified characteristics due to the temperature effect, centered on the upper face instead of cylinders. This will represent the continuity of the heating which begin at the top center of the plate before going deeper and wider.

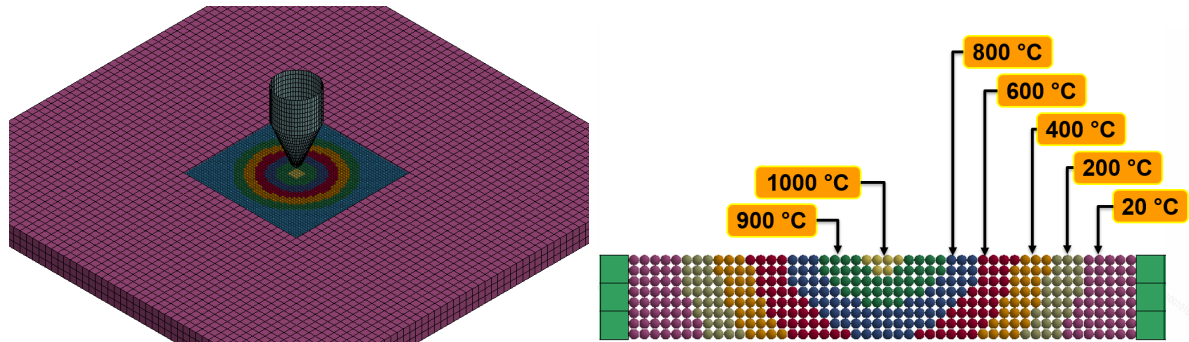Simultaneously, a new thermal test is done with the center temperature being at 1000°C instead of 800°C (figure 9).

Fig.7:   Isometric view and cutting plane of the spherical model with the new temperature zones

The results are enhanced and are more comparable to the experimental tests. As long as the plate isn't pierced, the SPH elements are pushed to the top of the plate through the weakened material. The displacement is helicoidal as the elements rise around the tool. These elements are well distributed around the piercing and create a smooth upper collar as expected by the experiment.

A last feature of the model is the lower associated stresses and strains. The maximum stress is reduced from 500 to 300 MPa and the high strain zone are concentrated around the drilling. Two reasons can explain this easier piercing of the plate: first, numerous elements are led by the tool to form the 2 mm height collar, permitting an easier displacement of the tool. Secondly, the temperatures at the center of the plate are higher and the matter deforms easily.
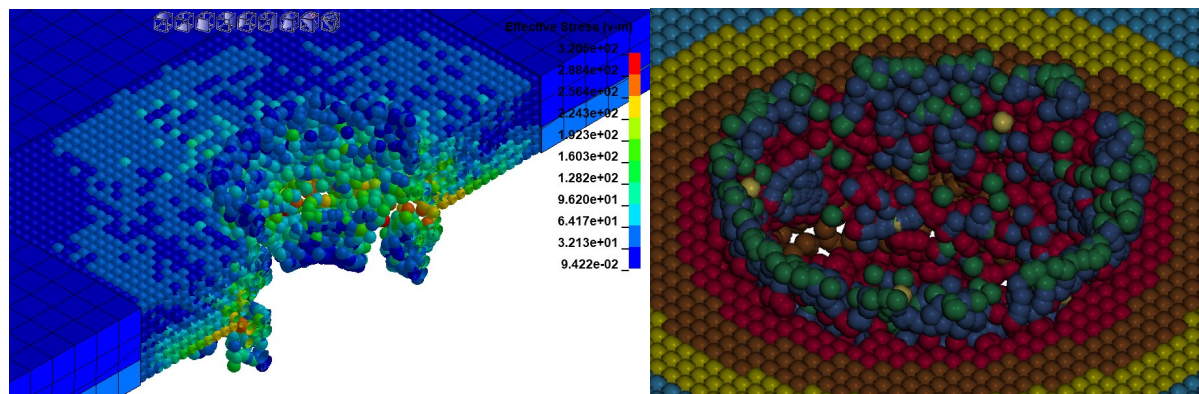

Fig.8:   Von Mises stress in MPa (left) and zoom on the upper side of the plate (right) at final time

The shape of the force curve is a little similar to the previous one: the spike is still shifted to the right. This highlights that the current simulation is still not accurate enough and that it will be needed to take into account the thermal effects properly in the future.

This model represents quite correctly the beginning of the flow drilling with the creation of the collar but the ending of the process simulation is flawed.
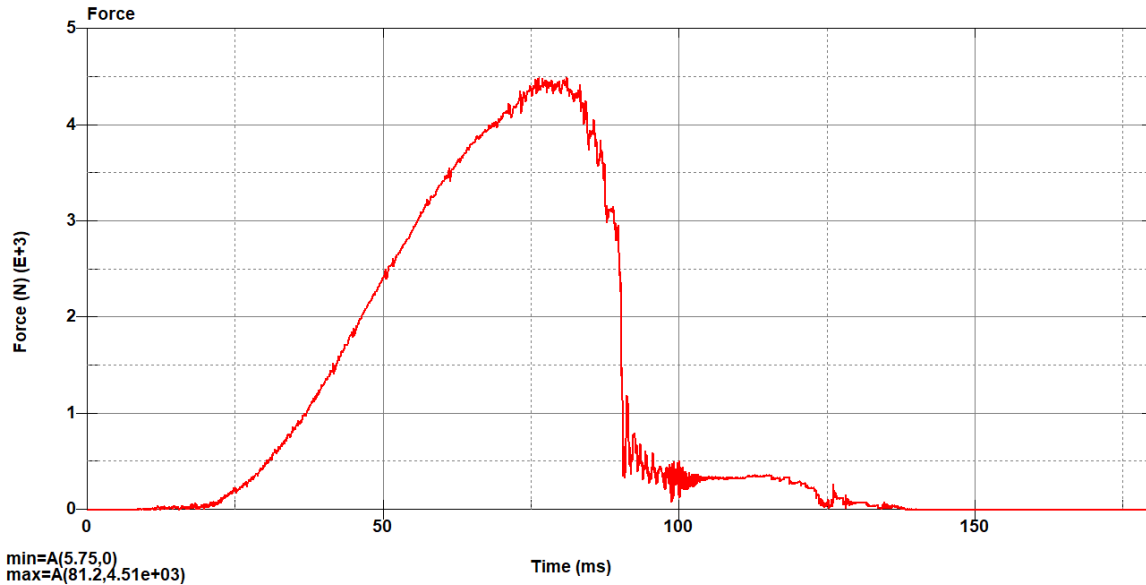
Fig.9:   Curve of the simulated thrust force

3.6   Experimental speed test

Now that the model is established, it is necessary to check if the same model with the experimental rotational and translational speeds will work properly. Such model will have a processing time 50 times higher, and thus is only launched for the final iteration.

The aim is to do a qualitative comparison of the behaviour of the fast model and the true model in order to check if the results of the fast model are correct enough.

There are some differences between the two models: the elements seem to turn around the tool even more in the model using the experimental speed. The collar itself is slightly different. Overall, the results are close and there is no absolute necessity to use the true speed model except for the final one.
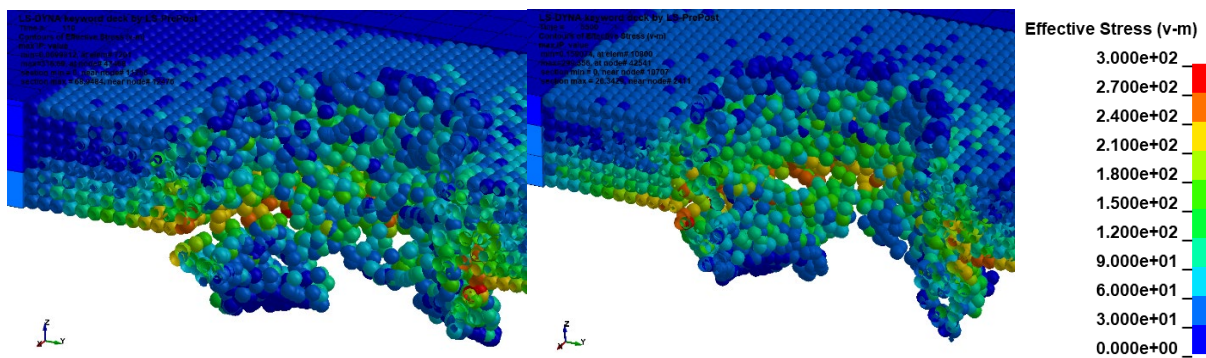

Fig.10: Comparison of the Von Mises Stress of the spherical gradients model at the end of the simulation between the fast model (left) and the true speed model (right)

4   Thermal approach

The following step consists in the integration of the thermal solver in the previous model. Beforehand, this phase requires the different constituent parts of the thermal model to be tested with the SPH method and to verify the availability of this parts before trying to implement them. This constituent parts are:
-    The thermal dilatation
-    The heat received by friction
-    The thermal diffusion
-    The thermal radiation

4.1   Material Law

From now on, the material law used for the S235 steel will be the Mat 106 (MAT_ELASTIC_VISCOPLASTIC_THERMAL) without using the kinetic hardening parameters. This new law uses curves to define the evolution of the parameters (Young modulus, Poisson coefficient, Elastic Strength, thermal dilatation…) against the temperature. [8] 23

A MAT_THERMAL_ISOTROPIC law is added. This law allows to add the lacking thermal parameters.

As in the previous case, the data are taken from the Eurocode 3. [04]

4.2   Thermal dilatation tests

The first thermal test aims to check the thermal dilatation with SPH elements. In order to do that, a simple simulation is created (figure 11): a 20 mm side cube of SPH elements (1000 elements) is surrounded by rigid parts (blue and red). The red part is fixed whereas the blue one can move only along the Z axis. A tied contact is set between the SPH part and the moving one and an automatic contact is set between the SPH part and the red one.

The temperature of the SPH elements slowly grows from 20 to 1000 °C. Thus, the dilatation of SPH elements will move the blue part and its movement will be monitored.
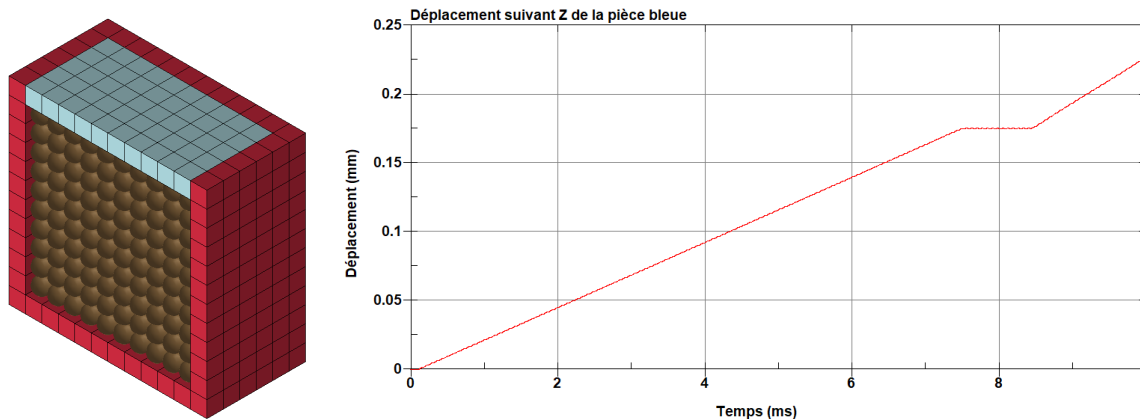

Fig.11: Sectional view of the model (left) and blue part displacement curve along the Z axis

The theoretical displacement distance caused by the thermal expansion is calculated at the moment of the flat level around 8 seconds (when the temperature is between 750 and 850 °C, the thermal expansion coefficient is null).
Between 20 and 750 °C, the thermal coefficient is equal to $12.e^{-6}$ mm/(mm.°C) [04] and the standard length of the cube is 20 mm; then displacement is equal to:

$$730 * (12.e - 6) * 20 = 0.1752\ mm$$

This calculus gives the same result as the simulation (Figure 11).

4.3 Friction tests

In order to check the good behaviour of the heat produced by friction with SPH elements, a simple model is realized. This model is made of two cubes of 10*10*5 mm³ made with standard finite elements (light blue) or in SPH elements (pink). These square move along a rigid plate of 60*40*2 mm³. Two tiles of 10*10*2 mm³ are tied to the upper side of the cubes and the movement and force are applied on these tiles in order to reduce the influence of the boundary conditions on the friction test. The movement is applied in order to move the cubes along the plate, producing a friction between these elements.

According to figure 12 the distributions of the temperatures after the displacement are close but not totally similar.
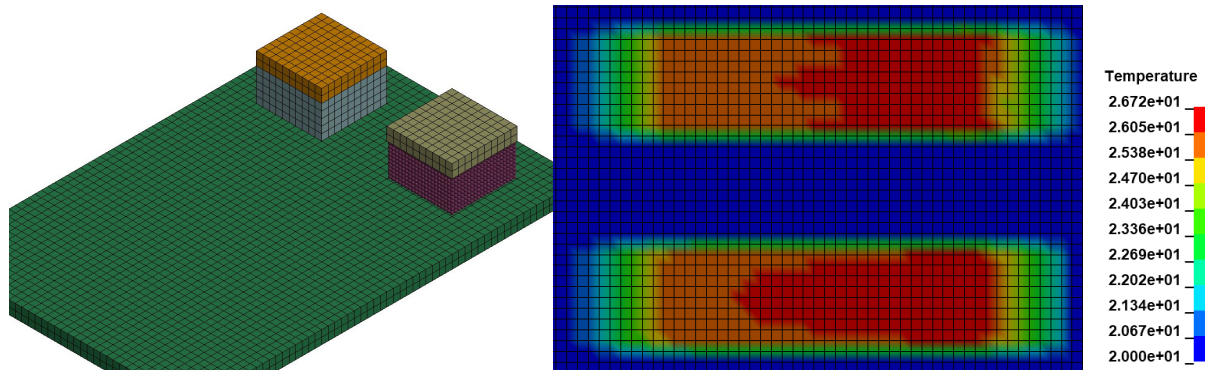

Fig.12: Model of the friction test (left) and the distribution of the temperature at the end of the friction (right)

However, the energies of friction are identical for both cubes. Globally, the distribution difference is marginal and will not be an issue for this case.
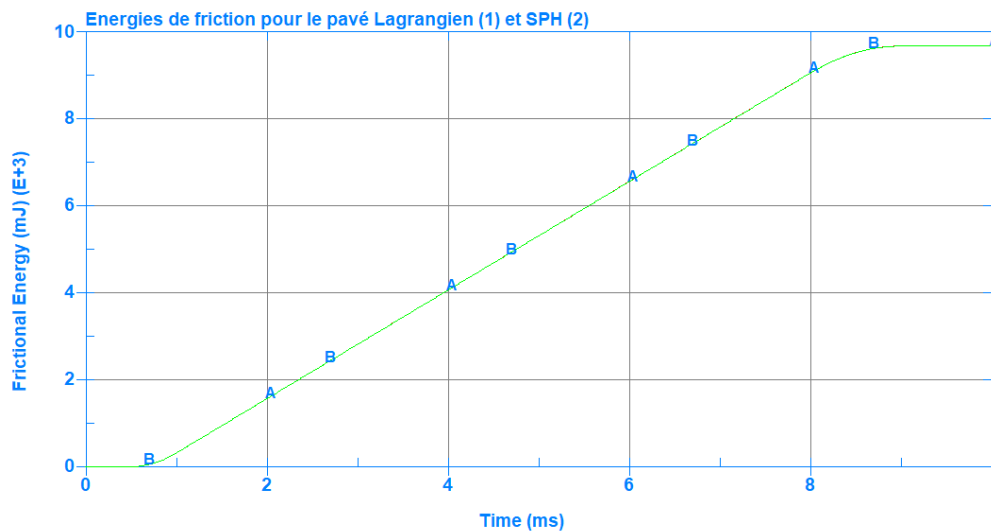

Fig.13: Friction energies of both cubes

4.4 Diffusion tests

The previous model is used to check the heat diffusion in SPH particles compared to the one in solid elements. By postponing the end of the simulation, the heat diffusion and its evolution can be evaluated. The distribution after a long period of time is globally similar. The only marginal difference is that the SPH elements have slightly more extreme temperatures. Such difference can be caused by the fact that the SPH elements meshing is coarser.
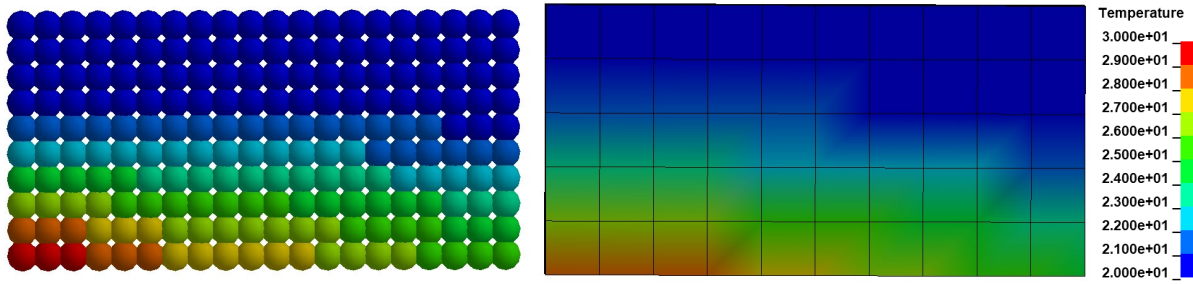
Fig.14: Gradient of temperature at the end of the simulation in the cube parts.

4.5   Heat transfer

Where the rubber hits the road is when radiative or conductive heat transfer with SPH elements has to be simulated (contact between SPH elements and the tool or the SPH surface and the air). LS-DYNA proposes some BOUNDARY_FLUX which works with SPH elements; it requires to create some segments between the SPH nodes which will suffer the flux. However, the SPH elements around the drilling, those who will suffer the flux, will be displaced during the simulation.

It seems there is no way to automatically detect the frontier of the SPH part as it is deformed. So, this feature can only be used after the drilling to check how the plate is cooling.

In order to ensure that the influence of the heat transfer is negligeable, an estimation of the power of the principal heat transfer between the tool and the plate is made and compared with the total energy created.
The power is at its maximum at the end of the process when the tool is at the highest temperature. For this estimation, the temperature of the tool is evaluated at 1500 °C while the plate in contact is at 800 °C. With such a difference, the convective flux is negligeable in regard to the radiative flux, only the last one will be calculated. With an emissivity of 0.8 and a contact surface of 43 mm² (a 2 mm tall and 3.5mm radius cylinder), the radiative flux can be calculated as such [XX] 11:

$$Q_{Rad} = \sigma * S * \varepsilon * \frac{(T1^4 - T2^4)}{(T1 - T2)} = 0.013 \, W$$

Concomitantly, the power of the friction force work is evaluated. The force itself is around 1000 N, the friction coefficient is around 0.2 and the displacement of the force is around 1.1 m/sec (a 3.5 mm radius circle is crossed at 3000 rpm).

$$W = F * k * V = 220 \, W$$

This result is far greater than the radiative flux, thus the heat transfer flux is negligeable in this regard during the process itself.

However, the thermal flux will be the main motor of the cooling process after the drilling itself. It will be necessary to simulate the heat transfer when investigating the evolution of the microstructure and heat treatment due to the cooling process.

4.6   Thermo-mechanical model

Now that the thermal tests have been done to ensure the good behaviour of the thermal features; there is to integrate thermal solver in the flow drilling model. The model is similar to the mechanical one: the plate is 100 mm long and 5 mm deep with the central area of 30 mm square being a SPH part. The bottom exterior nodes of the plate are clamped and the same model is used for the tool as previously. There is only one SPH part using a thermal material law.

The thermal features are gradually integrated in order to spot and repair every mistake. The first thermal feature is the MAT_THERMAL_ISOTROPIC_TD law alone. The tabulated law causes timestep issues,

reducing the timestep over and over. To fix this issue, the simpler MAT_THERMAL_ISOTROPIC is used, preventing the thermal dependency of the thermal capacity and of the thermal conductivity.

The analysis of the temperature's gradient (Figure 15) reveals that the temperature maximum in the plate is reached roughly in the middle of the simulation. Afterwards, it is supposed that the heated matter of the plate is soft enough to drill through it without much effort, reducing the friction force and energy, thus stopping the increase of temperature.

Additionally, the hypothesis of the spherical gradient is close to reality. The temperatures are higher around the top of the drilling especially in the upper contact with the tool, the SPH elements are pushed through these soft elements until the plate is pierced. Thus, these elements create a 2 mm height collar around the top of the hole.
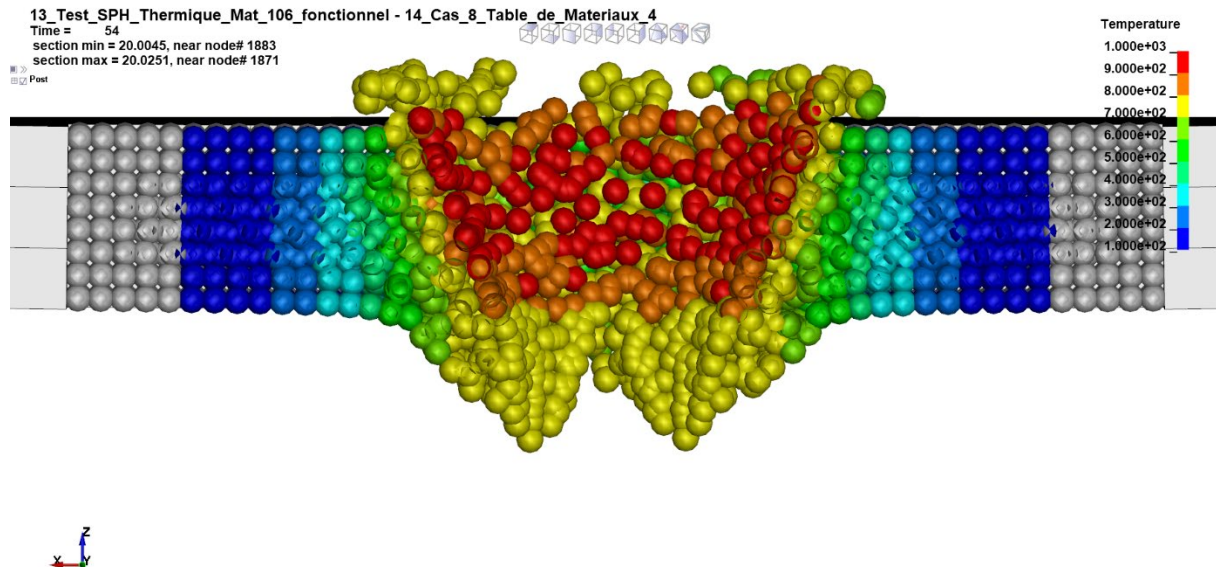

Fig.15: Gradient of temperature when the highest temperature is reached

This hypothesis is comforted by the Von Mises stress field in the plate at the same moment (Figure 16) which highlights how little the stress is in the heated area (25MPa).
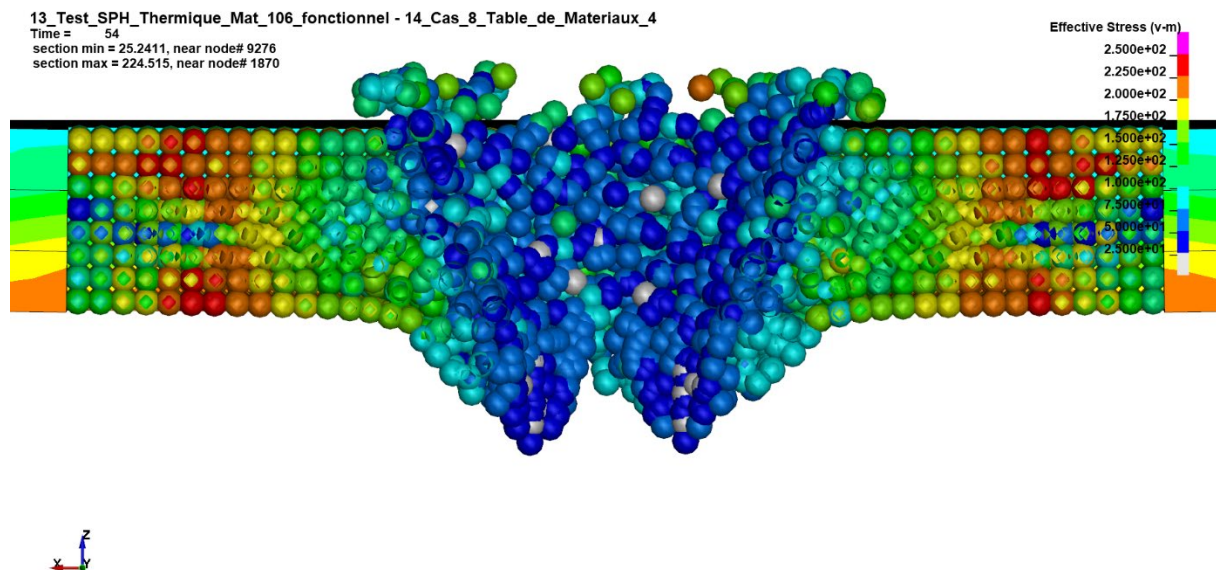

Fig.16: Von Mises stress of the thermal simulation when the highest temperature is reached

The force analysis (Figure 20) also consolidates this argument: the force required to go through the plate at constant speed reaches a peak at 9 kN around 31 ms and then slowly decreases as the matter becomes softer.

The shape of the curve is similar to those of the experimental literature. However, the magnitudes of the forces are still different: 9 kN in the simulation while around 1-2 kN in the literature. The source of this error could be the thickness difference with the experimental plate and the material characteristics.
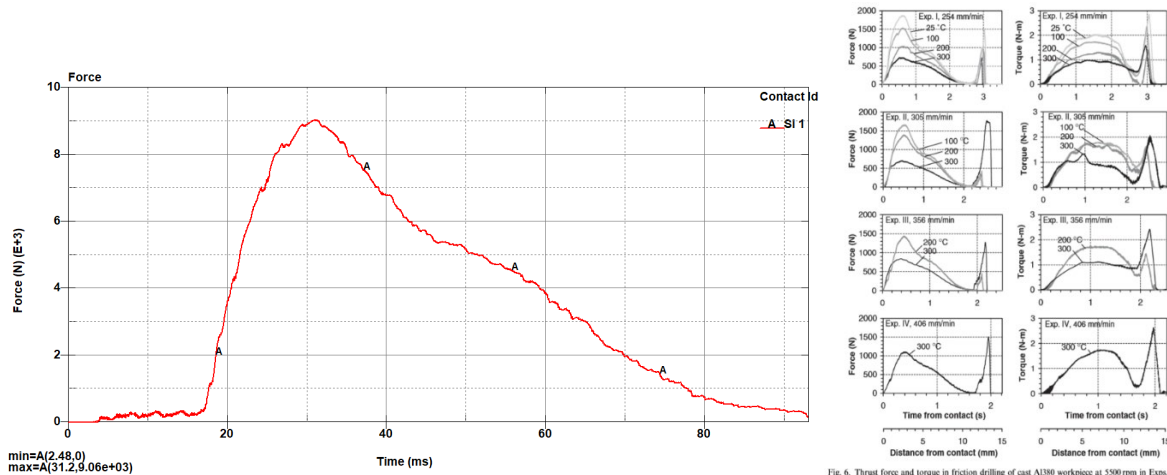

Fig.17: Curve of the simulated thrust force (left) compared to experimental thrust force and torque at different advance speed and pre-heated plate temperature (right)

There are still 4 petals, 5 mm height, forming. It is probably due to the geometry of the plate which guide the matter to form these petals. This assertion has to be verified with complementary tests with true thickness and more SPH elements in the depth. Such tests will also enable to confirm the reliability of the simplifications made in the previous models.

However, the present simulation takes 30 hours on 14 processors with a SMP executable; a more accurate test will require week long processing time without taking into account the increase in speed.

5   Conclusion

First and foremost, the mechanical model, even if highly simplified, showed positive results, correlating in some points with the reality. The experimental speed test gave really close results with the accelerated test; this leads to the possibility to work on a simplified model to enhance the simulation before using a more realistic model in order to obtain more accurate results.

The thermal tests had shown that most of the thermal features work properly with the SPH method; only the thermal contacts and heat transfers seem hard to manage with the SPH method.

Finally, the thermal modelling of the flow drilling process did give conclusive results that are closer to the reality than mechanical approaches; these encouraging results tend to testify the viability of the SPH method to simulate accurately the flow drilling process.

5.1   Perspectives

There are still many angles to study around the flow drilling process in order to enhance the simulation. First of all, it is certainly possible to do some simplifications on the model in order to reduce even more the processing time. It has been seen in the thermomechanical model that the highly deformed area is reduced compared to the one observed in the mechanical model; thus, the SPH area could be reduced. With such a little SPH area, the thermal transfer between the SPH and the rest of the plate has to be integrated in the model.

A test with the effective thickness of the plate has to be done to check if the results stay similar except the force necessary to go through the plate which should be reduced and if the magnitude of the force obtained is the same than in the literature.

By dividing by at least 2 the current processing time, it will be possible to realize tests with experimental speed and thickness.

A lot of characteristics (for example the friction coefficient) could be made more complex and be dependent of the temperature in order to accurately take into account various physical approaches.

In order to realize a realistic simulation of the process at true speed, true thickness and ideally with an increased accuracy, a lot more of resources are needed. Then experimental tests should be realized in order to calibrate the model and verify its accuracy to the reality. After the drilling simulation successfully emulates the reality, the following step would be to simulate the evolution of the microstructure of the steel, the cooling and the ensuing heat treatment.

6   Acknowledgements

7   Literature

[1]   « Friction drilling », *Wikipedia*. mars 30, 2020.

[2]   « Flowdrill - Flowdrill ». https://www.flowdrill.com/eu_fr/.

[3]   J. Sønstabø, « Behaviour and modelling of flow-drill screw connections », PhD Thesis, 2018.

[4]   COMITE EUROP DE NORMALISATION, « Eurocode 3: Design of steel structures - Part 1-2: General rules Structural fire design ».

[5]   S. F. Miller, A. J. Shih, et P. J. Blau, « Microstructural alterations associated with friction drilling of steel, aluminum, and titanium », *J. Mater. Eng. Perform.*, vol. 14, no 5, p. 647-653, oct. 2005.

[6]   S. F. Miller, J. Tao, et A. J. Shih, « Friction drilling of cast metals », *Int. J. Mach. Tools Manuf.*, vol. 46, no 12-13, p. 1526-1535, oct. 2006.

[7]   A. COL, « Emboutissage des tôles Aspect mécanique », *Techniques de l'ingénieur Mise en forme des métaux en feuilles*, vol. base documentaire : TIB191DUO., no ref. article : bm7511. Editions T.I., 2011.

[8]   LIVERMORE SOFTWARE TECHNOLOGY (LST), « LS-DYNA® KEYWORD USER'S MANUAL VOLUME II Material Models ».

[9]   A. Shapiro, « Using LS-DYNA for Heat Transfer & Coupled Thermal-Stress Problems ». Livermore Software Technology Corporation, 2012.

[10]   E. FEULVARCH, « Modélisation numérique du procédé de soudage par friction-malaxage », *Techniques de l'ingénieur Assemblage des matériaux par soudage*, vol. base documentaire : TIB512DUO., no ref. article : bm7764. Editions T.I., 2016.

[11]   Paul \AAkerström, « Modelling and Simulation of Hot Stamping », 2006.

[12]   V. K. Sarin, Éd., *Comprehensive hard materials*. Amsterdam: Elsevier, 2014.

[13]   LIVERMORE SOFTWARE TECHNOLOGY (LST), « LS-DYNA® KEYWORD USER'S MANUAL VOLUME I Material Models ».

[14]   F. Bremond, P. Fournier, et F. Platon, « Test temperature effect on the tribological behavior of DLC-coated 100C6-steel couples in dry friction », *Wear*, vol. 254, no 7-8, p. 774-783, avr. 2003.

[15]   S. F. Miller, J. Tao, et A. J. Shih, « Friction drilling of cast metals », *Int. J. Mach. Tools Manuf.*, vol. 46, no 12-13, p. 1526-1535, oct. 2006.